Diabetologia

Biomechanical and morphometric intestinal remodelling during experimental diabetes in rats

J. Zhao[1, 2]**, J. Yang**[1, 2]**, H. Gregersen**[1, 2, 3]

[1] Centre of Sensory-Motor Interaction, Aalborg University, Denmark
[2] Centre of Excellence in Visceral Biomechanics and Pain, Aalborg Hospital, Aalborg, Denmark
[3] Institute of Internal Medicine, University of Bergen, Norway

Abstract

Aims/hypothesis. Morphometric and passive biomechanical properties were studied in the duodenum, jejunum and ileum in 10 non-diabetic and 40 streptozotocin-induced diabetic rats.
Methods. The diabetic rats were divided into groups living 4 days, 1, 2, and 4 weeks after diabetes was induced ($n=10$ for each groups). The mechanical test was done as a ramp distension experiment. The intestinal diameter and length were obtained from digitised images of the intestinal segments at pre-selected pressures and at no-load and zero-stress states. Circumferential and longitudinal stresses (force per area) and strains (deformation) were computed from the length, diameter and pressure data and from the zero-stress state geometry.
Results. The blood glucose concentration increased four- to fivefold in the diabetic rats. Streptozotocin-induced diabetes generated pronounced increase in the weight per centimetre length, wall thickness and wall cross-sectional area in all intestinal segments during diabetes ($p<0.05$). Histological analysis showed that the thickness of the intestinal layers was increased in all segments during diabetes ($p<0.05$). In the duodenum the opening angle did not change in the first 2 weeks and decreased after 4 weeks ($p<0.05$). In the jejunum and ileum the opening angle increased after 1 week in the diabetic group. The residual strain showed the same pattern as the opening angle. Furthermore, it was found that the circumferential and longitudinal stiffness of the intestinal wall increased with the duration of diabetes ($p<0.05$ and $p<0.01$).
Conclusion/interpretation. Morphological and biomechanical remodelling of the small intestine occurred during the development of diabetes. [Diabetologia (2003) 46:1688–1697]

Keywords STZ-induced diabetes, intestine, morphometry, stress-strain, stiffness, zero-stress state.

Diabetes mellitus is defined as a chronic disease characterised by metabolic disorders with fasting hyperglycaemia and glycosuria [1]. The main metabolic complications of diabetes are retinopathy, nephropathy and peripheral vasculopathy. Gastrointestinal (GI) disorders are common among diabetic patients. As many as 75% of patients visiting diabetes clinics report GI symptoms [2, 3]. The entire GI tract can be affected by diabetes mellitus. Common complaints include dysphagia, early satiety, reflux, constipation, abdominal pain, nausea, vomiting, and diarrhoea. Both acute and chronic hyperglycaemia can lead to specific GI complications. As with other complications of diabetes, the duration of the disease and poor glycaemic control seem to be associated with the severity of GI problems.

Streptozotocin (STZ), the most potent diabetogenic agent, has been widely used to induce experimental diabetes in rats since it causes alterations similar to those found in diabetic humans [4]. Diabetes induced

by STZ is characterised by morphological GI remodelling such as proliferation of different layers, especially of the mucosa in the small intestine [5, 6, 7, 8, 9, 10]. Because morphological remodelling of the small intestine occurs in diabetes, the biomechanical properties are also likely to change. Biomechanics deals with the relation between stress (force per area) and strain (deformation) which expressed the stiffness of the tissue. Residual stress and strain are the difference in stress and strain between the no-load (without any external forces applied) and zero-stress state (no external and internal forces).

Only sparse data about the relation between the passive biomechanical properties and the diabetic intestine have been reported. One study showed that diabetes altered the tension-strain relation of the small intestine in a way consistent with stiffening of the intestinal wall [10]. In recent years, the passive biomechanical properties of the normal and diseased intestinal wall have been studied extensively in humans and animals [11, 12, 13, 14, 15, 16, 17, 18, 19]. We consider the zero-stress state, residual strain and stress-strain relationship of the intestinal wall as the relevant quantitative remodelling parameters because they are measures of the non-uniformity of growth or resorption in different parts of the intestinal wall. We have shown previously that the opening angle and residual strain were lower in the duodenum and larger in the jejunum and ileum in diabetic rats compared to normal rats [20]. However, no data on the stress-strain distribution of the intestinal wall referenced to the zero-stress state in diabetes have been reported.

The aim of this study was to investigate the biomechanical and morphometric properties of the small intestine in diabetic rats. The study focuses on the time-dependent changes in morphometry and stress-strain properties of intestinal segments in STZ-induced diabetic rats with reference to the zero-stress state.

Materials and methods

A total of 50 male Wistar rats, 2 to 3 months old, and weighing 200 to 240 g, were used in this study. Approval of the protocol was obtained from the Danish Committee for Animal Experimentation. Of these rats, 40 were made diabetic by a single intraperitoneal injection of 50 mg/kg STZ (Sigma-Aldrich Denmark A/S, Vallensbæk Strand, Denmark) and were divided into four groups that lived for 4 days (d4), 1 week (W1), 2 weeks (W2), and 4 weeks (W4) (n=10 in each group), respectively. Another ten rats of similar age and body weight from the same vendor were used as control animals (N). The body weight of control and diabetic rats was measured at the beginning of the experiment, and afterwards at 1-week intervals. Blood glucose was examined at the beginning and at the end of each experiment.

Experimental procedures. The experimental procedures are similar as those reported by us before [16, 17, 18, 19, 20, 21]. Briefly, after 4 days, 1, 2 and 4 weeks, respectively, the animals were anaesthetised with sodium pentobarbital (50 mg/kg, ip). The calcium antagonist, papaverine (60 mg/kg) was used

to abolish contractile activity in the GI tract. Three 6-cm-long segments from duodenum (duo), jejunum (jej) and ileum (ile) were harvested. The duodenum was taken from the descending part, 1 cm down from the pylorus; the jejunum from 5 cm distal to the ligament of Treitz, and the ileum from 5 cm proximal to the ileo-cecal valve. Then the segments were placed immediately into calcium-free Krebs solution containing 6% dextran and 0.25% EGTA. The solution was aerated with a gas mixture of 95% O_2-5% CO_2 at pH 7.4. From each end of the segments, a 1-cm-long tissue was cut and fixed in 4% formalin for histological examination. The two rings both from the proximal and distal ends of the intestinal segments were used for no-load state and zero-stress state analysis. One end of the remaining segment was tied with a suture and the other end was cannulated with a tube for the distension experiment. After preconditioning the intestinal segments, they were inflated with Krebs solution using a ramp distension protocol from 0 to 8 cmH$_2$O (0–0.8 kPa) for duodenum and jejunum and from 0 to 6 cmH$_2$O for ileum at a rate of 2 cm/min. The outer diameter and the length were recorded for each 0.5 cmH$_2$O pressure level. The intestinal segments conformed to a cylindrical geometry during the distensions.

For obtaining data on the zero-stress state, the intestinal rings were collected as mentioned above and placed in the Krebs solution. A photograph was taken of the cross-section of the rings in the no-load state. Then each ring-shaped segment was cut radially when immersed in the fluid under the microscope. Each ring opened up into a sector. Photographs were taken about 30 min after the radial cutting to allow viscoelastic creep to take place.

Histology. Each intestinal sample for histology was fixed in 10% buffered formalin over 24 h, Then, the specimen was dehydrated in a series of graded ethanol (70%, 96% and 99%) and embedded in paraffin. Five-micron sections were cut perpendicular to the mucosa surface and the paraffin was cleared from the slides with coconut oil (over 15 min at 60°C). The sections were redehydrated in 99%, 96% and 70% ethanol followed by a 10-min wash in water and stained with haematoxylin and eosin. The thickness of the different layers in all segments was measured by the same pathologist in a blinded review. For the layer thickness measurements, twelve determinations were made on each specimen and averaged. Microscopic examination was only carried out on sections where the total wall thickness could be observed.

Mechanical data analysis. The morphometric data were obtained from digitised images of the segments in the zero-stress, no-load and pressurised states. Measurements were undertaken using image analysis software (Sigmascan ver. 4.0, Sigma, San Rafael, Calif., USA). The following data were measured from each specimen: the circumferential length (C), the wall thickness (h), the wall area (A), and the opening angle at zero-stress state (α). The subscripts i, o, n, z and p refer to the inner (mucosal) surface, outer (serosal) surface, no-load state, zero-stress state and pressurised condition. The opening angle α was defined as the angle subtended by two radii drawn from the midpoint of the inner wall to the inner tips of two ends of the specimen. Furthermore, the outer diameter (D) and the length (L_p) were measured from the images of the pressurised segments.

The measured data was used to compute biomechanical parameters defined as:

Residual Green's strain at the mucosal surface:

$$E_i = \frac{\left(\frac{C_{i-n}}{C_{i-z}}\right)^2 - 1}{2} \tag{1}$$

Residual Green's strain at the serosal surface:

$$E_o = \frac{\left(\frac{C_{o-n}}{C_{o-z}}\right)^2 - 1}{2} \tag{2}$$

Residual strain difference:

$$E_{difference} = E_o - E_i \tag{3}$$

Residual strain difference normalised to the wall thickness:

$$\frac{E_{difference}}{h} \tag{4}$$

The stress and strain of the intestine in the pressurised state were computed under the assumption that the wall was homogenous and the intestinal shape was cylindrical. Calculation was done from knowing the no-load state dimensions, the outer diameters and lengths of the specimen at varying pressures, and assuming incompressibility of the intestinal wall. The longitudinal stretch ratio, $\lambda_\phi = \frac{L_p}{L_z}$; the luminal radius, $r_{i-p} = \sqrt{r_{o-p}^2 - \frac{A_n}{\pi\lambda_\phi}}$; the wall thickness, $h_p = r_{o-p} - r_{i-p}$; the mucosal circumferential length, $C_{i-p} = 2 \times \pi \times r_{i-p}$; the serosal circumferential length, $C_{o-p} = 2 \times \pi \times r_{o-p}$; the mid-wall circumferential length, $C_{m-p} = \frac{C_{i-p} + C_{o-p}}{2}$; the circumferential stretch ratio, $\lambda_\theta = \frac{C_{m-p}}{C_{m-z}}$ (where the middle-wall circumferential length at zero-stress state, $C_{m-z} = \frac{C_{i-z} + C_{o-z}}{2}$) were computed. Then the Kirchhoff's stress and Green's strain in an intestinal wall at a given pressure were computed according to the following equations:

Circumferential Kirchhoff's stress:

$$S_\theta = \frac{\Delta P r_{i-p}}{h_p \lambda_\theta^2} \tag{5}$$

Longitudinal Kirchhoff's stress:

$$S_\phi = \frac{\Delta P r_{i-p}^2}{h_p \lambda_\phi^2 (r_{o-p} + r_{i-p})} \tag{6}$$

Circumferential midwall Green's strain:

$$E_\theta = \frac{\lambda_\theta^2 - 1}{2} \tag{7}$$

Longitudinal Green's strain:

$$E_\phi = \frac{\lambda_\phi^2 - 1}{2} \tag{8}$$

ΔP is the transmural pressure difference. The longitudinal midwall stretch ratio was referenced to the no-load state because tissue strips could not be cut for obtaining the zero-stress state in longitudinal direction. However, the longitudinal mid-wall length in rat intestine does not differ between the no-load and zero-stress states [21].

We assume the intestinal wall to be an incompressible, non-linearly elastic orthotropic material subjected to finite deformation. The biaxial stress and strain of the intestine fitted to the strain energy function in a two-dimensional analysis [22].

$$P_0 W = \frac{C}{2} e^Q \tag{9}$$

Where

$$Q = \left[a_1\left(E_\theta^2 - E_\theta^{*2}\right) + a_2\left(E_\phi^2 - E_\phi^{*2}\right) + 2a_4\left(E_\theta E_\phi - E_\theta^* E_\phi^*\right)\right] \tag{10}$$

P_0 is the material density of the intestinal wall (mass per unit volume). W is the strain energy per unit mass. E_θ^* and E_ϕ^* are reference strains measured at a physiological pressure, and C, a_1, a_2, and a_4 are material coefficients. Under assumptions that materials in a wall are homogeneous and pseudoelastic, the stress components can be expressed as:

$$S_\theta = \frac{\partial(\rho_0 W)}{\partial E_\theta} \tag{11}$$

$$S_\phi = \frac{\partial(\rho_0 W)}{\partial E_\phi} \tag{12}$$

By substituted eqs. 9 and 10 into eqs. 11 and 12, the following stress-strain relations for the intestinal segments in both the circumferential and longitudinal directions can be obtained:

$$S_\theta = C\left(a_1 E_\theta + a_4 E_\phi\right)e^Q \tag{13}$$

$$S_\phi = C\left(a_4 E_\theta + a_2 E_\phi\right)e^Q \tag{14}$$

where E_θ^*, E_ϕ^* are strains corresponding to a standard pair of stresses S_θ^*, S_ϕ^*. A Marquardt's non-linear, least-squares algorithm was used to fit the experimental data, and the coefficients and C, a_1, a_2, and a_4 were calculated by minimising the sum of the squares of the differences between the experimental and computed data.

Statistical analysis. The data were representative of a normal distribution and accordingly the results were expressed as means ± SEM. The constant a_1 and a_2 from the above exponential functions were used for the statistical evaluation of the stress-strain data. Analysis of variance was used to detect possible variations in axial direction of the small intestine and the differences of different parameters in different groups (Sigmastat 2.0). In case of statistical significance, data were evaluated in pairs by a multiple comparison procedure (Student-Newman-Keuls method). If the normality test or the equal variance test failed, Kruskal-Wallis one-way analysis of variance on ranks was used. Linear regression analysis was used to show possible association between the biomechanical and morphometric parameters. The results were regarded as significant when p was less than 0.05.

Results

Basic data. The control rats gained weight continuously ($p<0.01$) whereas the diabetic rats lost weight in the first week and then maintained a relatively stable weight (Fig. 1a). The blood glucose concentration increased from the normal value (~10 mmol/l) to 40.3±8.7 mmol/l 4 days after STZ was injected (Fig. 1b). After 4 weeks the blood glucose concentration reached 49.3±6.6 mmol/l. The whole intestine (Fig. 2a, F=56.2, $p<0.001$) and the wet weight per unit length of all three segments (Fig. 2b) increased during the development of diabetes (duodenum, F=22.8, $p<0.001$; jejunum, F=33.3, $p<0.001$; ileum, F=34.3, $p<0.001$).

Morphometry data. The wall thickness and wall area of the intestinal segments gradually increased during the development of diabetes (Table 1). Statistical significance was reached after 2 weeks of diabetes (wall thickness, duodenum, F=13.6, $p<0.001$, jejunum,

Table 1. Wall thickness and cross-sectional wall area (mean ± SEM)

	No-load state wall thickness (mm)			Zero-stress state wall thickness (mm)			No-load state wall area (mm^2)		
	Duodenum	Jejunum	Ileum	Duodenum	Jejunum	Ileum	Duodenum	Jejunum	Ileum
N	1.09±0.02	0.81±0.02	0.57±0.01	1.09±0.02	0.80±0.02	0.59±0.01	9.87±0.21	6.17±0.25	5.98±0.21
d4	1.19±0.02	0.87±0.02	0.58±0.01	1.21±0.02	0.84±0.02	0.59±0.01	11.35±0.39	6.77±0.35	6.01±0.21
W1	1.22±0.01	0.93±0.02	0.65±0.02	1.23±0.01	0.93±0.02	0.65±0.01	12.36±00.49	7.25±0.23	6.49±0.25
W2	1.29±0.03	1.03±0.02	0.74±0.02	1.30±0.03	1.03±0.02	0.77±0.01	13.04±0.65	8.59±0.23	8.32±0.37
W4	1.34±0.04	1.07±0.02	0.76±0.02	1.33±0.04	1.08±0.02	0.79±0.02	14.23±0.66	8.71±0.34	9.07±0.32

The wall thickness and wall area of intestinal segments gradually increased with the duration of diabetes. See the text for statistical analysis
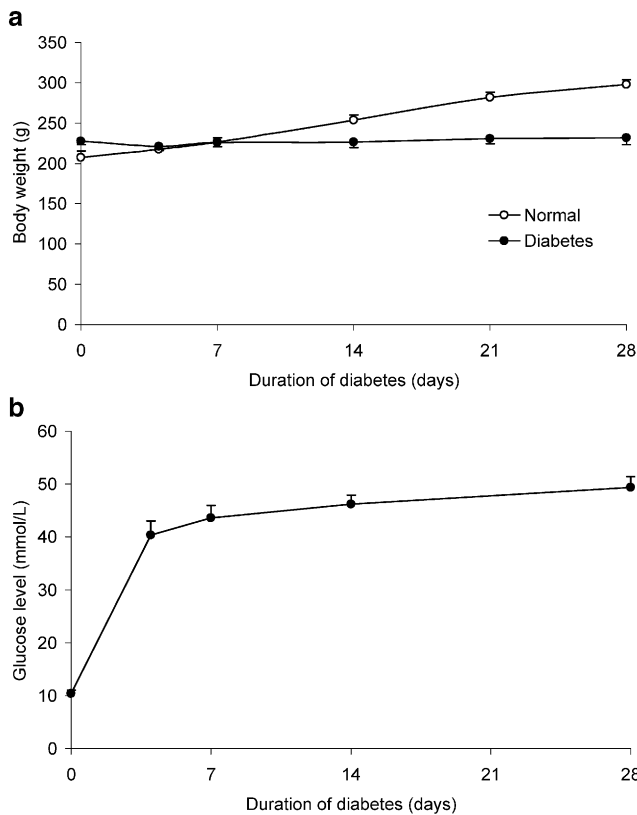
Fig. 1a, b. The body weight (**a**) and blood glucose concentration (**b**) in the control and streptozotocin-induced diabetic rats (Mean ± SEM)

Fig. 2a, b. The weight of whole intestine (**a**) and the wet weight per unit length of all three segments (**b**) (Mean ± SEM)

F=27.8, $p<0.001$ and ileum, F=33.4, $p<0.001$; wall area, duodenum, F=13.1, $p<0.001$, jejunum, F=15.5, $p<0.001$ and ileum, F=26.7, P<0.001). The outer diameter increased as a function of the transmural pressure in all intestinal segments and groups. An increase in the outer diameter was found during the development of diabetes (duodenum, F=583.6, $p<0.001$, jejunum, F=407.4, $p<0.001$ and ileum, F=370.3, $p<0.001$). The wall thickness-to-inner radius ratio increased as function of the transmural pressure during the development of diabetes (duodenum, F=101.4, $p<0.001$, jejunum, F=221.6, $p<0.001$ and ileum,
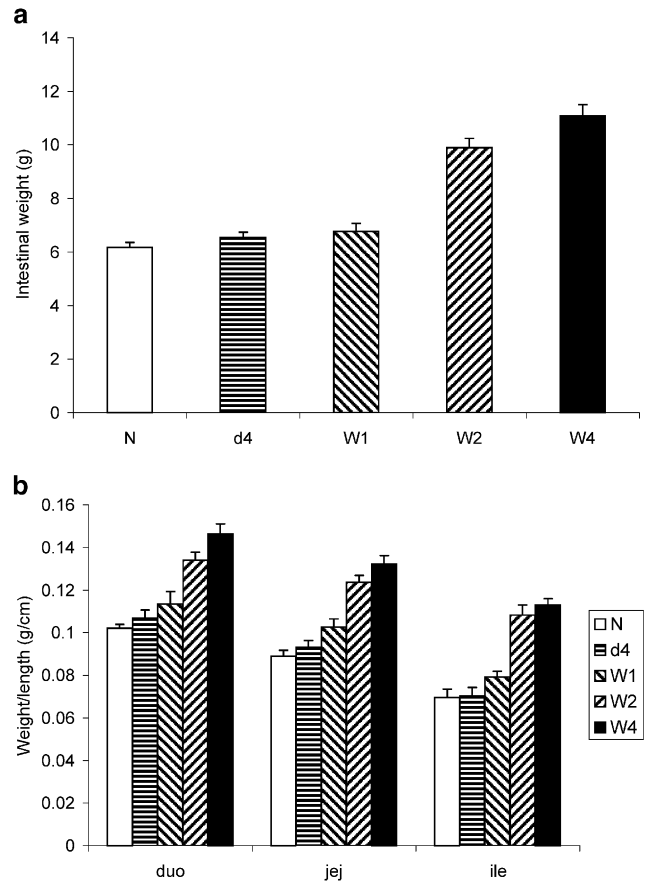
F=103.9, $p<0.001$). Figure 3 shows the outer diameter and wall thickness-to-inner radius ratio as a function of transmural pressure for the duodenum.

The outer and inner circumferential lengths at no-load and zero-stress states were longer in duodenal and jejunal segments of diabetic rats after 2 weeks whereas only 4 weeks later in ileal segments compared to those of the controls (Table 2) (F>3.3 and $p<0.05$ for all).

Histological data. The villus height (Fig. 4a), crypt depth (Fig. 4b), mucosa thickness (Fig. 4c), submu-

Table 2. Circumferential length (means ± SEM) (mm)

		Inner no-load	Outer no-load	Inner zero-stress	Outer zero-stress
Duodenum	N	5.11±0.22	12.33±0.13	8.55±0.14	10.98±0.13
	d4	5.31±0.33	13.28±0.31	9.51±0.47	11.77±0.29
	W1	5.33±0.21	13.64±0.31	9.49±0.34	11.72±0.23
	W2	5.59±0.34	14.13±0.34	11.79±0.38	13.26±0.44
	W4	6.85±0.19	15.36±0.28	12.59±0.41	13.99±0.36
Jejunum	N	5.26±0.15	10.93±0.21	7.84±0.13	9.96±0.26
	d4	5.11±0.37	10.95±0.39	7.74±0.44	10.16±0.44
	W1	5.42±0.25	11.25±0.25	7.94±0.21	10.06±0.21
	W2	5.72±0.29	12.71±0.30	9.01±0.35	11.62±0.35
	W4	6.14±0.25	12.74±0.37	9.61±0.41	11.49±0.41
Ileum	N	7.62±0.38	11.62±0.35	8.89±0.31	11.01±0.39
	d4	7.67±0.25	11.68±0.27	9.51±0.29	10.79±0.26
	W1	7.99±0.27	11.96±0.25	9.78±0.21	10.96±0.24
	W2	8.72±0.34	13.68±0.26	11.49±0.22	12.73±0.21
	W4	9.47±0.36	14.56±0.29	12.61±0.29	13.39±0.25

The outer and inner circumferential lengths at no-load and zero-stress states were longer in diabetic rats compared with the control rats. See the text for statistical analysis
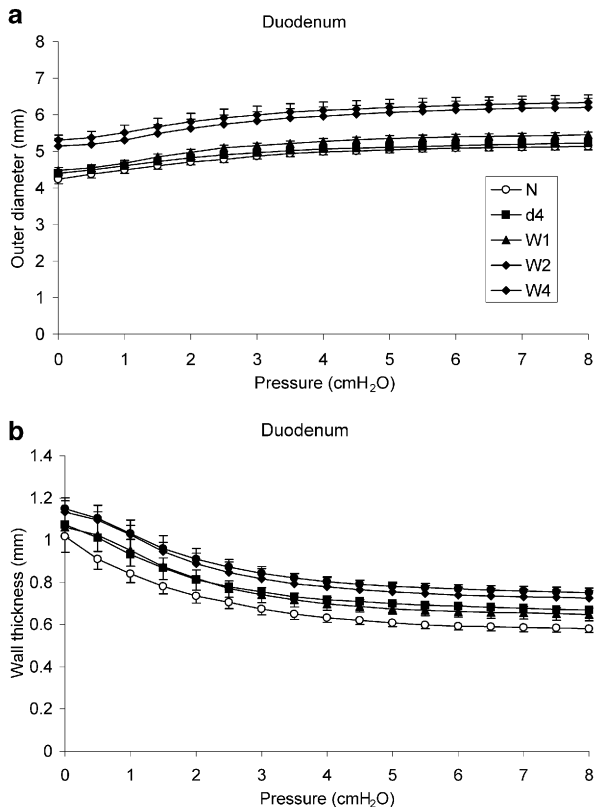
Fig. 3a, b. Mean ± SEM of outer diameter (*left*) and wall thickness-to-inner radius ratio (*right*) as function of pressure for the normal and the four diabetic groups on duodenal segment. Significant differences in outer diameter and wall thickness-to-inner radius ratio with the duration of diabetes treatment were found

cosa thickness (Fig. 4d), muscle thickness (Fig. 4e) and whole wall thickness (Fig. 4f) increased during diabetes. The differences were found after 7 days of diabetes for most parameters ($p<0.05$). Especially the

mucosa layer thickness had a pronounced increase, i.e. increasing after 4 days of diabetes in the duodenum and after 7 days of diabetes in the jejunum and ileum ($p<0.01$).

Biomechanical data. The opening angles and residual strains of the intestinal segments are shown in Fig. 5. In brief, the opening angle did not change significantly in the first 2 weeks in the duodenal and jejunal segments. Thereafter it decreased in the duodenum (F=3.6, $p<0.05$) and increased in the jejunum (F=5.3, $p<0.05$). The opening angle was increased after 4 days of diabetes in the ileum (F=13.9, $p<0.01$). The residual strain of the mucosal surface was compressive whereas the serosal residual strain was tensile. The same patterns as the opening angle were found for the residual strain at the mucosa and serosa (inner residual strain, duodenum, F=2.6, $p<0.05$; jejunum, $p>0.05$; ileum, F=3.0, $p<0.05$; outer residual strain, $p>0.05$ for all segments).

The circumferential and longitudinal stress-strain relations are shown in Fig. 6. In the circumferential direction, the stress-strain curves were different among the three segments during the development of diabetes. In the duodenum, the stress-strain curve shifted to the left during experimental diabetes. The difference was found after 1 week of diabetes (F=9.89, $p<0.01$). In the jejunum, the curve shifted to the right after 1 week of diabetes. Thereafter, it returned to the normal state again and shifted to the left after 4 weeks of diabetes (F=7.83, $p<0.01$). In the ileum, no differences were found during the first 2 weeks, After that the stress-strain curve shifted to the left indicating that the stiffness increased (F=3.3, $p<0.05$). In longitudinal direction, the stress-strain curve tended to shift to the left 1 week after injection of STZ in all segments. The difference was found 1
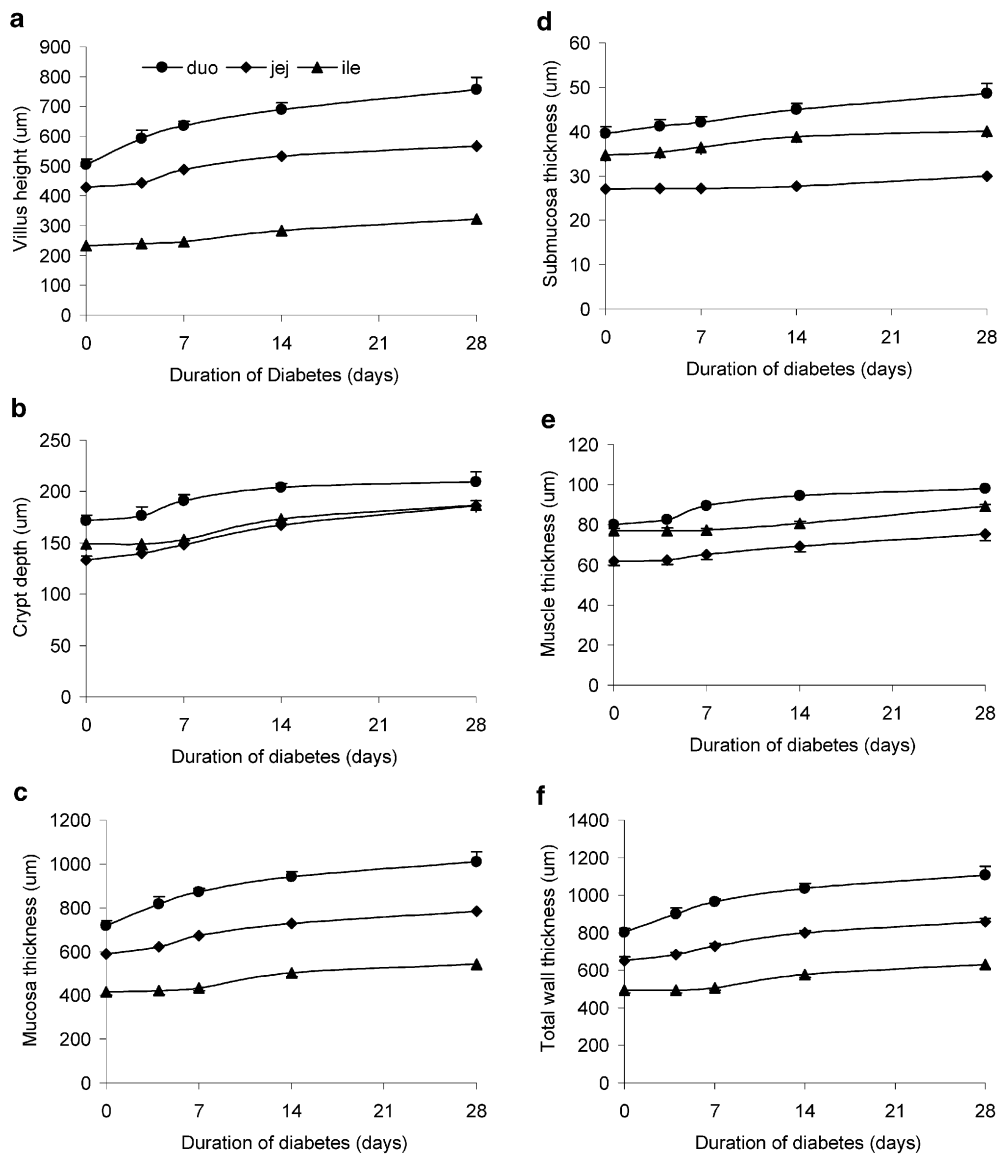
Fig. 4a–f. Means ± SEM of the villus height (**a**), the crypt depth (**b**), and the thickness of mucosa (**c**), submucosa (**d**), and muscle (**e**) and total wall thickness (**f**). All parameters in-creased during the development of diabetes with the most pro-nounced increase in the mucosa layer

Table 3. The average constants of two-axial stress-strain analysis in different segments of the intestine (fixed a_4=0.5, average ± SEM)

|		N	4d	W1	W2	W4
Duodenum	a_1	4.97±0.86	5.69±1.18	5.89±0.61	6.83±0.98	8.12±0.96
	a_2	8.07±2.05	8.99±1.39	9.32±2.18	9.56±1.94	11.79±1.41
	C	0.19±0.07	0.14±0.02	0.12±0.02	0.16±0.03	0.14±0.03
Jejunum	a_1	2.71±0.54	2.79±1.01	2.71±0.55	2.79±0.43	3.81±0.34
	a_2	6.19±2.17	6.92±1.53	8.55±2.18	8.53±1.43	9.92±1.67
	C	0.19±0.04	0.31±0.09	0.21±0.06	0.19±0.03	0.17±0.04
Ileum	a_1	1.88±0.713	1.91±0.43	1.91±0.36	2.09±0.32	3.05±0.48
	a_2	2.94±0.93	3.85±0.94	4.18±0.68	5.14±0.95	6.11±1.06
	C	0.39±0.13	0.33±0.11	0.29±0.09	0.31±0.09	0.28±0.09
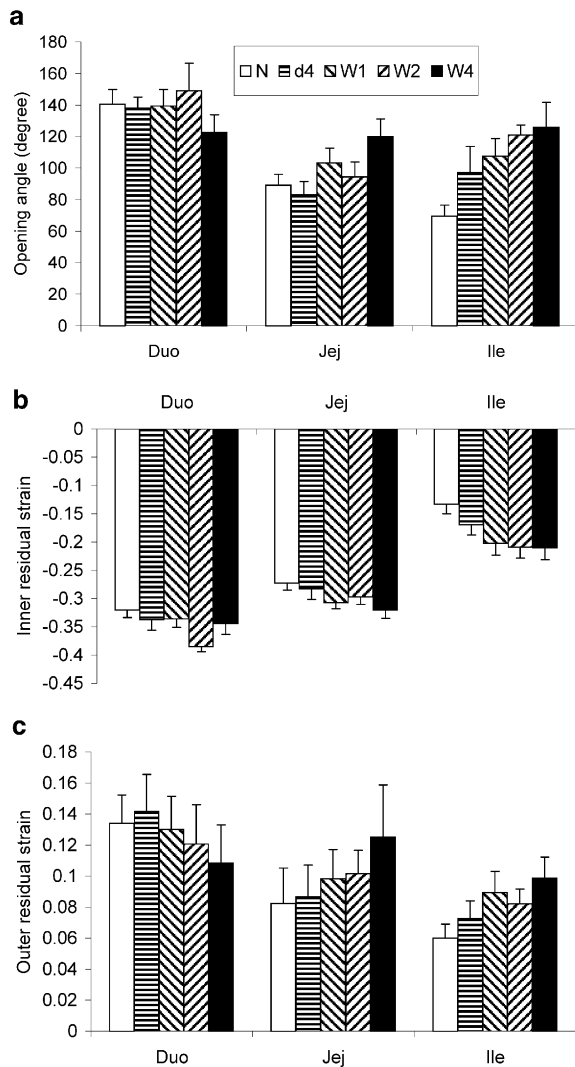
Fig. 5a–c. Means ± SEM of the opening angle (**a**) and corresponding inner (**b**) and outer (**c**) residual strains during the development of diabetes. The opening angles did not change significantly before 2 weeks in duodenal and jejunal segments, thereafter decreased in the duodenum and increased in the jejunum. The opening angle was increased after 4 days of diabetes in the ileum. The same patterns were found for residual strain at the mucosa and serosa

week after the STZ injection in the duodenum and jejunum and after 2 weeks in the ileum when compared with the control group (duodenum, F=4.69, $p<0.05$; jejunum, F=6.44, $p<0.05$; ileum F=13.04, $p<0.01$). The results of the two-axial stress-strain analysis are given in Table 3. The constant a_1 and a_2 were increased with the development of experimental diabetes in all segments.

Discussion

Hyperglycaemia due to relative or absolute lack of insulin and the development of diabetes-induced intestinal change characterise all types of diabetes mellitus

[1, 2]. Studies of the gut in the STZ model of diabetes have almost entirely involved the use of the rat. To evaluate the results from our study, certain aspects of this model of diabetes mellitus need to be considered. The form of diabetes mellitus induced by parenteral streptozotocin administration in rats is insulin-dependent (Type 1). Without treatment with insulin, STZ-induced diabetic rats become hyperglycaemic, polyphagic, polidipsic, poliuric and undernourished. In this study, the blood glucose concentration was four to five times higher in diabetic rats than in non-diabetic rats. Many studies have shown that experimental Type 1 diabetes causes morphological, functional, and metabolic alterations in the small intestine [2, 3, 5, 6, 7, 8, 9, 10, 23]. The major findings in this study were that the opening angle and residual strain were lower in the duodenum and larger in the jejunum and ileum in diabetic rats compared to normal rats. Stress-strain relationship analysis showed that both in the circumferential and longitudinal directions the stiffness of the intestinal wall increased with the duration of diabetes. Furthermore, we confirmed previous data that the intestinal weight, weight-per-unit length and wall thickness and area increased in the diabetic rats.

The changes in the opening angle of the intestine during diabetes shown in the previous study [20] and in this study suggest that the morphological and biomechanical remodelling of different layers are an important determinant of the zero-stress state. Fung's hypothesis of non-uniform remodelling states that if the inner wall grows more than the outer wall, the opening angle will increase; whereas if the outer wall grows more than the inner wall, the opening angle will decrease [24]. In this experiment, since the changes in jejunum and ileum during the diabetes primarily are in the mucosa layers, the inner wall grows more than the outer wall and hence the opening angle increased. Correspondingly, the outer residual strain became more tensile whereas the inner residual strain became more compressive in these two segments. However, in the duodenal segment, the opening angle and absolute value of residual strain decreased during diabetes. We noted that all layers of duodenum increased after experimental diabetes. At this condition the biomechanical properties of layers can determine the remodelling of the zero-stress state. With increased wall stiffness, it is likely that the opening angle becomes smaller.

To understand the tissue forces in the gastrointestinal tract, it is necessary to know the stress-strain relationships of the tissues. The stress-strain distribution mainly reflects the elastic properties of the intestine. The elastic property changes reflect the structural remodelling of the intestinal wall during the diabetic development. Another study showed that diabetes alters the tension-strain relation of intestine in a way consistent with a stiffer wall [10]. However, in that study the biomechanical properties analysis was not referenced to the zero-stress state, and the longitudinal stress-
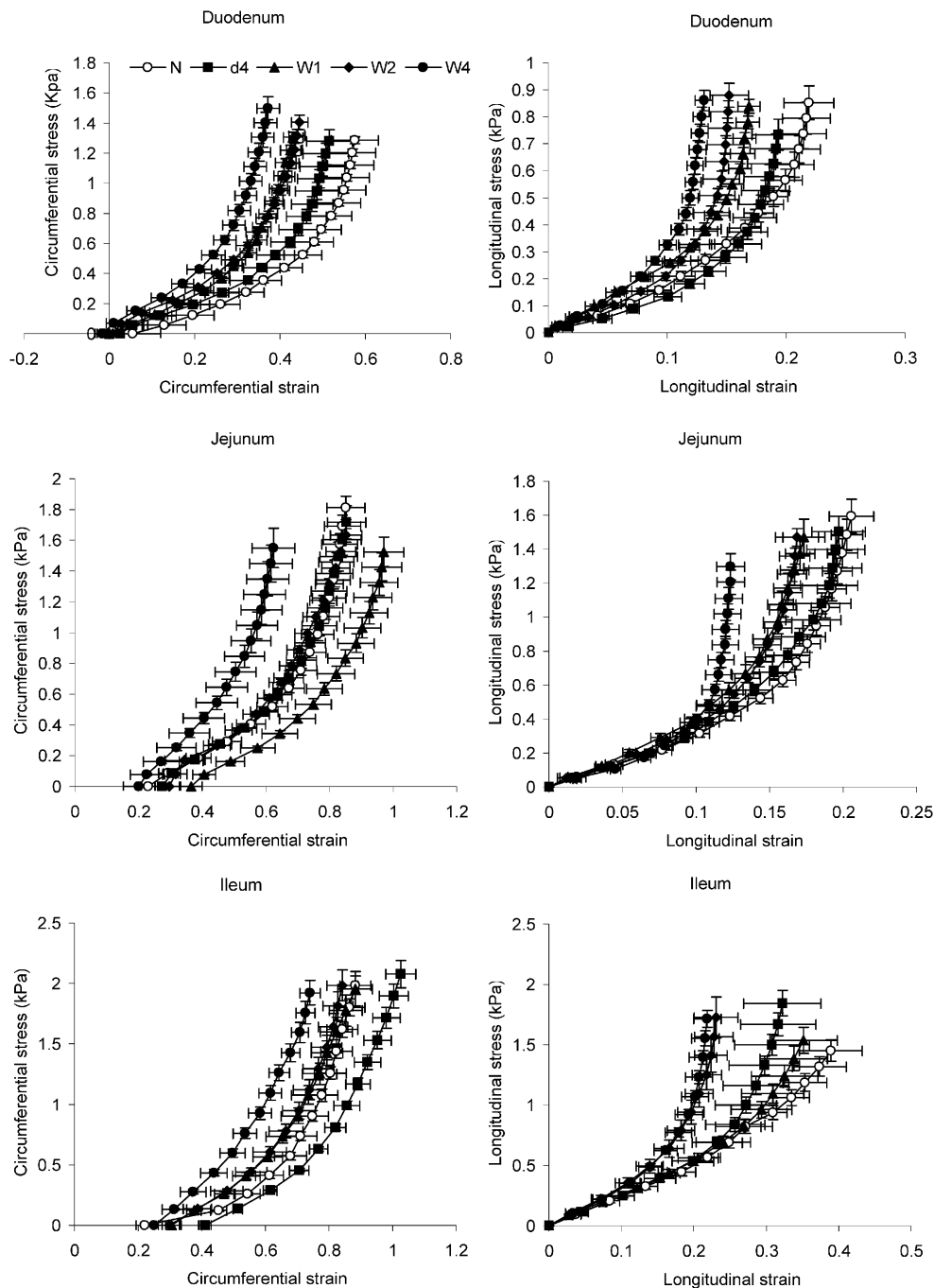
Fig. 6. (Mean ± SEM) of the relation between circumferential (*left*) and longitudinal (*right*) stress and strain. In the circumferential direction, the stress-strain curve of duodenum shifted to the left after the development of experimental diabetes; the significant difference was found after 1 week of the experiment. The curves of jejunum and ileum shifted to the right after 1 week of diabetes, thereafter it shifted to the left indicating that the stiffness increased. In the longitudinal direction, 1 week after injection of STZ in all segments the curves shift to the left. A statistically significant difference was found 1 week after injection of STZ in the duodenum and jejunum and 2 weeks in ileum compared with the control group

strain relationship was not obtained. Our study improved these deficiencies. The biaxial stress-strain analysis provided the mechanical constants C, a_1, a_2, and a_4. The meaning of the material constants was discussed in detail [22]. Constant a_1 is the elastic modulus in the circumferential direction that affects the curve for S_θ vs E_θ, the higher a_1, the stiffer the intestine wall in circumferential direction. Constant a_2 is the elastic modulus in the longitudinal direction that affects the curve for S_l vs E_l in a similar way. Constant a_4 is the cross modulus, and constant C fixes the scale on the stress axis. The larger the value of a_1, a_2 and a_4, the smaller the C value becomes. Our study shows that both the circumferential and longitudinal

stiffness of the intestinal wall increased with the duration of diabetes. However, no evidence of which structure in the wall causes the increased stiffness was found. Alterations in the orientation, configuration, and content of collagen are likely candidates based on remodelling studies in other disease models and because collagen in most tissues is the stress-bearing structure [25]. Some studies on the arteries and diabetes have shown that the non-enzymatic glycation of collagen have a close relation with the increased arterial wall stiffness [26, 27, 28]. We believe that this also appies to the collagen in the intestinal wall. A study has shown a thickening of the colonic subepithelial collagen layer in diabetic patients [29]. We postulate that a close relation between the intestinal collagen glycation and intestinal passive biomechanical properties exists.

Untreated diabetic rats eat two to three times as much as the control rats, and this hyperphagia could possibly account for the observed intestinal growth seen in these animals [30]. However, diabetic rats fed with the same isocaloric diet as that of the control rats still exhibit greater small bowel mass and enhanced crypt cell DNA synthesis [31, 32]. This indicates that at least part of the growth response of intestinal adaptation in diabetes is independent of increased nutrient consumption. The mechanism by which hyperphagia stimulates intestinal growth is not clear. One study showed increased concentrations of both plasma and tissue glucagon-like peptide 2 (GLP-2) that correlate with intestinal growth and adaptation to STZ diabetes. Furthermore, both the increase in GLP-2 concentrations and the bowel growth response were reverted by insulin therapy. Of interest, the increments in plasma concentrations of GLP-2 preceded any changes in intestinal weight, thereby providing further evidence for a relationship between GLP-2 and the induction of intestinal growth in diabetes [33]. Their study supports the idea that an increased nutrient load could stimulate release of hormones trophic to the intestine. The combination of hyperphagia and increased gastric emptying [31] observed in diabetic rats results in a greater nutrient load being delivered to the small intestine. Because luminal nutrients, including fat and carbohydrate, are physiological L-cell secretagogues in vivo [34, 35], this provides a possible mechanism whereby increased luminal nutrients stimulate release of GLP-2 into the circulation thereby exerting a trophic action on the intestinal epithelium. It is also well known that the epithelial homeostasis is balanced by regulating cell proliferation and cell death. The active form of caspase-3 was attenuated 1 week after streptozotocin treatment. Suppression of apoptosis in the early days of STZ-induced diabetes was responsible for the increased mucosal height in the small intestine in STZ-induced diabetic animals [23]. The GLP-2 also inhibit apoptosis in the small intestine [36]. Although no direct evidence of intestinal mucosa proliferation was

reported on human diabetic patients, small bowel hypertrophy was described in a patient carrying a proglucagon-expressing tumour that secreted the intestinal PGDPs [37].

In these experiments, the diabetes-induced intestinal remodelling shows axial variation. The reason could be due to the axial differences in morphology and passive biomechanical properties in the small intestine. Previous studies have shown the different passive biomechanical properties among the duodenal, jejunal and ileal segments of the intestine [17, 21, 27, 28]. The differences in biomechanical properties are probably associated with the specialised functions of the proximal and distal segments of the small intestine. The duodenum has large influence on gastric emptying and has been proposed to act as a capacitate resistor whereas the distal ileum acts as a reservoir. In the duodenum, the phasic contractions are more prevalent, the transit of luminal contents is quicker than in the distal ileum, and the duodenal wall is thicker than that of the ileum [18, 26]. The non-homogeneous changes in residual strain, opening angle and stress-strain relation observed in this experiment can be associated with the common complaints, including dysphagia, early satiety, reflux, constipation, abdominal pain, nausea, vomiting, and diarrhoea, that are found in the diabetic patients.

References

1. Renold AE, Mintz DH, Muller WA, Cahill GF (1978) Diabetes mellitus. In: Stanbury JB, Wyngaarden JB, Freidrickson D (eds) The metabolic basis of inherited diseases. McGraw-Hill, New York, pp 89–91
2. Folwaczny C, Riepl R, Tschop M, Landgraf R (1999) Gastrointestinal involvement in patients with diabetes mellitus: Part I (first of two parts). Epidemiology, pathophysiology, clinical findings. Z Gastroenterol 37:803–815
3. Verne GN, Sninsky CA (1998) Diabetes and the gastrointestinal tract. Gastroenterol Clin North Am 27:861–874
4. Ar'Rajab A, Ahren B (1993) Long-term diabetogenic effect of streptozotocin in rats. Pancreas 8:50–57
5. Zoubi SA, Williams MD, Mayhew TM, Sparrow RA (1995) Number and ultrastructure of epithelial cells in crypts and villi along the streptozotocin-diabetic small intestine: a quantitative study on the effects of insulin and aldose reductase inhibition. Virchows Arch 427:187–193
6. Mayhew TM, Carson FL, Sharma AK (1989) Small intestinal morphology in experimental diabetic rats: a stereological study on the effects of an aldose reductase inhibitor (ponalrestat) given with or without conventional insulin therapy. Diabetologia 32:649–654
7. Zoubi SA, Mayhew TM, Sparrow RA (1995) The small intestine in experimental diabetes: cellular adaptation in

crypts and villi at different longitudinal sites. Virchows Arch 426:501–507

8. Tahara T, Yamamoto T (1988) Morphological changes of the villous microvascular architecture and intestinal growth in rats with streptozotocin-induced diabetes. Virchows Arch A Pathol Anat Histopathol 413:151–158

9. Charlton M, Ahlman B, Nair KS (2000) The effect of insulin on human small intestinal mucosal protein synthesis. Gastroenterology 118:299–306

10. Jørgensen CS, Ahrensberg JM, Gregersen H, Flyvberg A (2001) Tension-strain relation and morphometry of rat small intestine in experimental diabetes. Dig Dis Sci 46: 960–967

11. Storkholm JH, Villadsen GE, Jensen SL, Gregersen H (1995) Passive elastic wall properties in isolated guinea pig small intestine. Dig Dis Sci 40:976–982

12. Gregersen H, Kassab G (1996) Biomechanics of the gastrointestinal tract. Neurogastroenterol Mot 8:277–297

13. Gregersen H, Kassab G, Pallencaoe E et al. (1997) Morphometry and strain distribution in guinea pig duodenum with reference to the zero-stress state. Am J Physiol 273: G865–G874

14. Gao C, Zhao J, Gregersen H (2000) Histomorphology and strain distribution in pig duodenum with reference to the zero-stress state. Dig Dis Sci 45:1500–1508

15. Gregersen H, Kassab GS, Fung YC (2000) The zero-stress state of the gastrointestinal tract: biomechanical and functional implications. Dig Dis Sci 45:2271–2281

16. Dou YL, Gregersen S, Zhao JB, Zhuang FY, Gregersen H (2001) Effect of re-feeding after starvation on biomechanical properties in rat small intestine. Medical Eng Phys 23:557–566

17. Zhao JB, Sha H, Zhuang FY, Gregersen H (2002) Morphological properties and residual strain along the small intestine in rats. World J Gastroenterol 8:312–317

18. Dou Y, Gregersen S, Zhao J, Zhuang F, Gregersen H (2002) Morphometric and biomechanical intestinal remodeling induced by fasting in rats. Dig Dis Sci 47:1158–1168

19. Dou Y, Lu X, Zhao J, Gregersen H (2002) Morphometric and biomechanical remodeling in the intestine after small bowel resection in the rat. Neurogastroenterol Motil 14: 43–53

20. Zhao JB, Sha H, Zhou SP, Tong XL, Zhuang FY, Gregersen H (2002) Remodelling of the zero-stress state of the small intestine in streptozotocin-induced diabetic rats. Effect of Gliclazide. Dig Liver Dis 34:707–716

21. Dou Y (2001) Aspects of morphometric and biomechanical properties in the normal, the fasting, the refeeding and the resected rat small intestine. Thesis, Aalborg University, Denmark

22. Fung YC, Fronek K, Patitucci P (1979) Pseudoelasticity of arteries and the choice of mathematical expression. Am J Physiol 237:620–631

23. Noda T, Iwakiri R, Fujimoto K et al. (2001) Suppression of apoptosis is responsible for increased thickness of intestinal mocosa in streptozotocin-induced diabetic rats. Metabolism 50:259–264

24. Fung YC (1991) What are the residual stresses doing in our blood vessels. Ann Biomed Eng 19:237–249

25. Fung YC (1993) Biomechanics. Properties of living tissues. Springer-Verlag, Berlin

26. Monnier VM, Glomb M, Elgawish A, Sell DR (1996) The mechanism of collagen cross-linking in diabetes: a puzzle nearing resolution. Diabetes 45 [Suppl 3]:S67–S72

27. Sims TJ, Rasmussen LM, Oxlund H, Bailey AJ (1996) The role of glycation cross-links in diabetic vascular stiffening. Diabetologia 39:946–951

28. Wolffenbuttel BH, Boulanger CM, Crijns FR et al. (1998) Breakers of advanced glycation end products restore large artery properties in experimental diabetes. Proc Natl Acad Sci USA 95:4630–4634

29. Kandemir O, Utas C, Gonen O et al. (1995) Colonic subepithelial collagenous thickening in diabetic patinets. Dis Colon Rectum 38:1097–1100

30. Jervis EL, Levin RJ (1966) Anatomic adaptation of the alimentary tract of the rat to the hyperphagia of chronic alloxan-diabetes. Nature 210:391–393

31. Granneman JG, Stricker EM (1984) Food intake and gastric emptying in rats with streptozotocin-induced diabetes. Am J Physiol 247:R1054–R1061

32. Miller DL, Hanson W, Schedl HP, Osborne JW (1977) Proliferation rate and transit time of mucosal cells in small intestine of diabetic rat. Gastroenterology 73:1326–1332

33. Fischer KD, Dhanvantari S, Drucker DJ, Brubaker PL (1997) Intestinal growth is associated with elevated levels of glucagon-like peptide 2 in diabetic rats. Am J Physiol 273:E815–E820

34. D'Alessio D, Thirlby R, Laschansky E, Zebroski H, Ensinck J (1993) Response of tGLP-1 to nutrients in humans. Digestion 54:377–379

35. Roberge JN, Brubaker PL (1991) Secretion of proglucagon-derived peptides in response to intestinal luminal nutrients. Endocrinology 128:3169–3174

36. Drucker DJ (2002) Biological actions and therapeutic potential of the glucagon-like peptides. Gastroenterology 122:531–544

37. Gleeson MH, Bloom SR, Polak JM, Henry K, Dowling RH (1971) Endocrine tumour in kidney affecting small bowel structure, motility, and absorptive function. Gut 12: 773–782